S28-32
185088

TDA Progress Report 42-114

August 15, 1993

N94-14397

HRMS Sky Survey Wideband Feed System Design for DSS 24 Beam Waveguide Antenna

P. H. Stanton, P. R. Lee, and H. F. Reilly
Ground Antennas and Facilities Engineering Section

The High-Resolution Microwave Survey (HRMS) Sky Survey project will be implemented on the DSS 24 beam waveguide (BWG) antenna over the frequency range of 2.86 to 10 GHz. Two wideband, ring-loaded, corrugated feed horns were designed to cover this range. The horns match the frequency-dependent gain requirements for the DSS 24 BWG system. The performance of the feed horns and the calculated system performance of DSS 24 are presented.

I. Introduction

The High-Resolution Microwave Survey (HRMS) project includes a sky survey over the frequency range of 1 to 10 GHz. The DSS 24 34-m beam waveguide (BWG) antenna will be used from 2.86 to 10 GHz; for frequencies below this, DSS 24 is unsuitable and another antenna will be utilized. To minimize complexity and expense, two wideband feed horns were designed to cover this broad frequency range on DSS 24. The performance of the horns was analyzed, and the upper-frequency horn was built and tested. The system performance of the horns installed on DSS 24 was also analyzed using computer software.

II. Feed-Horn Design

Two wideband conical feed horns were designed covering the frequency ranges of 2.86 to 5.35 GHz and 5.34 to 10 GHz. These ranges were chosen to match those of the upper-band HRMS orthomode transitions. A wideband feed horn for the DSS 24 BWG antenna needs to track specific gains and phase-center locations versus frequency to obtain high antenna efficiency and low spillover noise. Curves were fitted to the existing DSN narrowband designs for DSS 24 at 2.1625 GHz, 7.8725 GHz, and 33.25 GHz, and used as initial design values for the HRMS horns. Figure 1 shows these curves. The wideband (approximately 1:1.9) HRMS feeds for the DSS 24 antenna were matched to the fitted gain curve using the Gaussian beam model in [1] by adjusting the horn output flare angle and the aperture diameter. Fortunately, these wideband HRMS BWG feed designs adequately track the desired phase-center location versus frequency curve.

Once the horn output flare angle and the aperture diameter were determined, the detailed design followed the one presented in [2]. The horn parameters used in the design of the HRMS BWG feed horns are listed in Table 1. Figure 2 shows the four sections of the horn design: ring-loaded mode converter, frequency transition, angle transition, and output flare. Figures 3(a) and 3(b) show profiles

of the 2.86- to 5.35-GHz horn and the 5.34- to 10-GHz horn, respectively.

III. Horn Fabrication

The corrugated horn beyond the mode converter was fabricated using computer numerical control (CNC) lathe techniques. This procedure uses a computer-generated program written and checked on plotters before fabrication begins. It reduces the possibility of human error caused by repetitious movement.

The ring-loaded slot mode converter section at the horn input (see Fig. 2) presented a different problem. With the ring-loaded grooves, the mode converter section is impossible to fabricate as a single unit on conventional equipment. Several fabrication techniques were investigated. The cost, tolerance, and ability to make minor changes were the drivers in choosing the technique used. Each ring-loaded slot was split down the center, and half of each slot was machined into adjacent disks (Fig. 4). All of the disks had the same precise outside diameter. A holder with a precision bore and length was fabricated to align and compress these disks. Interfaces between the horn, the holder, and the disks were treated like typical waveguide joints. This design allows changes to individual ring-loaded slots by changing disks.

IV. Horn Performance

The horns were analyzed with a JPL computer program.[1] The program uses field matching techniques to determine the scattering matrices of the transverse electric (TE_{mn}) and transverse magnetic (TM_{mn}) modes of the horns [3]. From the scattering matrices, the aperture mode fields and the return loss of the horns are known. The radiation patterns of the horns can be calculated from the aperture mode fields by using the radiation integral.

The calculated gain and near-field phase-center location of the horns versus the frequency are shown in Figs. 5 and 6, along with the initial design gain and phase-center location. The calculated gain is somewhat higher than the initial design gain because of the approximation of the Gaussian beam model used in [1]. Computer analyses on DSS 24 revealed that the higher gain provided better noise temperature performance than the initial design gain but still had a comparable gain-to-noise temperature ratio (G/T).

[1] D. J. Hoppe, *Scattering Matrix Program for Ring-Loaded Circular Waveguide Junctions* (unnumbered, internal document), Jet Propulsion Laboratory, Pasadena, California, August 3, 1987.

The upper-frequency horn has been built and tested. The lower-frequency horn has been fabricated, but has not been fully tested. The return loss of the upper-frequency horn was measured on a Hewlett Packard 8510C network analyzer. The measured return loss, along with the calculated return loss of both horns, is shown in Fig. 7. Far-field radiation patterns of the upper-frequency horn were measured on JPL's Mesa Antenna Range at several frequencies from 5.34 to 11 GHz. The copolarization measurements matched the calculated patterns very well. Figure 8 compares one typical measurement with the calculated pattern. The maximum measured cross-polarization signal is 32.6 dB below the peak copolarization signal within the operating band of 5.34 to 10 GHz. The maximum error between the measured and the calculated values is 4.4 dB. Figure 9 shows the measured values for the 5.34- to 10-GHz horn, and the calculated values for both horns.

V. DSS 24 Performance

The performance of the DSS 24 BWG antenna with the HRMS feeds was predicted by using JPL computer programs[2] based on physical optics (PO) and physical optics/Jacobi-Bessel (POJB) techniques [4,5]. These programs are numerically intensive and consume large amounts of computer time. They were run on the JPL Cray Y-MP2E supercomputer, Voyager.

With the PO program results, it is possible to calculate the total spillover power of the BWG reflectors, the subreflector, and the main reflector. For the spillover power of the BWG mirrors, an effective noise temperature value of 280K was used in the pedestal room, and a value of 230K was used in the shroud above the pedestal room.[3] The effective noise temperature values for the spillovers past the main and subreflectors were taken to be 240K and 5K, respectively, for the antenna at zenith.

To find the best physical positions of the feeds, several feed locations were analyzed until the peak G/T was found. Five frequencies in each feed operating band were examined. The optimal position for each feed varies less than 23 cm over its frequency band. By locating the feeds in the center of their respective optimal position ranges,

[2] R. E. Hodges and W. A. Imbriale, *Computer Program POMESH for Diffraction Analysis of Reflector Antennas* (unnumbered, internal document), Jet Propulsion Laboratory, Pasadena, California, February 1992.

[3] W. Veruttipong and M. Franco, "A Technique for Computation of Noise Temperature Due to a BWG Shroud," JPL Interoffice Memorandum 3328-92-0149, Rev. A (internal document), Jet Propulsion Laboratory, Pasadena, California, November 3, 1992.

less than 0.05 dB/K is lost and the feed horns do not need to be relocated during operation.

To place the feeds in the pedestal room of DSS 24, a flat plate must be used with each feed. The 5.34- to 10-GHz horn will fit in the available space with its axis vertical and a flat plate above it (Fig. 10). However, the 2.86- to 5.35-GHz horn will not fit so easily. The horn will be placed with its axis horizontal, which, unfortunately, causes extra wear on the low-noise-amplifier refrigeration vacuum pump. Figure 11 shows the configuration of the horn and the mirror.

Beam squint was examined at the highest and lowest frequencies in both horn bands by running both right-circular and left-circular polarizations (RCP and LCP) of the horn patterns through the PO programs. The tilt angle varied from 6 millidegrees at 2.86 GHz to 2 millidegrees at 10 GHz. The tilt angle to half-power beamwidth ratio remained fairly constant, varying from 0.031 to 0.034. The loss due to squint ranged from 0.011 dB at 2.86 GHz to 0.013 dB at 10 GHz.

Major RF system requirements[4] are listed in Table 2. Table 3 shows the calculated system performance for the antenna at zenith, including noise temperature,[5] aperture efficiency, beam efficiency, gain,[6] G/T, and target G/T.[7]

VI. Conclusions

Two HRMS Sky Survey wideband (approximately 1:1.9) feed horns were designed to be compatible with the DSS 24 BWG antenna, covering a combined frequency range of 2.86 to 10 GHz. The upper-frequency horn has been fabricated and tested. The RF measurements were in close agreement with the calculated values in both the radiation patterns and return loss. Based on the results of the upper-frequency horn, the performance of the lower-frequency horn is expected to closely match the calculated performance.

The predicted DSS 24 aperture efficiency is greater than 0.747 over this frequency range. At the lower end of each of the two feed-horn frequency ranges, the noise temperature is higher than the 25 K maximum required. The predicted G/T, however, is at least 0.3 dB greater than is required over the entire frequency range. The beam efficiency is in the range of 0.772 to 0.881, short of the $\geq$0.9 requirement. The beam efficiency could be improved at the expense of the aperture efficiency.

A DSN frequency in the HRMS 2.86- to 10-GHz range available for comparison is 8.45 GHz (X-band). The design expectations of DSS 24 for DSN operation at 8.45 GHz, excluding the S-/X-band dichroic plate, are 0.766 aperture efficiency and 24.20 K noise temperature.[8] For the HRMS design at 8.45 GHz, substituting the DSN estimated values for the DSN preamplifier assembly for the HRMS preamplifier assembly, an aperture efficiency of 0.732 and a noise temperature of 23.16 K are predicted. The HRMS design has a resulting G/T of 54.56 dB/K compared to 54.57 dB/K for the DSN design.

[4] G. A. Zimmerman, *Search for Extra-Terrestrial Intelligence — Microwave Observing Project Sky Survey Element*, JPL 1720-4100 (internal document), Jet Propulsion Laboratory, Pasadena, California, November 12, 1991.

[5] The noise temperature includes contributions from the sky and atmosphere, reflector spillover, reflector ohmic losses, main reflector leakage, horn ohmic losses, scattering from the subreflector support structure, and the low-noise amplifier (LNA) assembly. Sky and atmosphere and LNA assembly values from: JPL-ARC Front-End Design Team, *NASA SETI Common Radio Frequency System Design Team Report* (internal report), Appendix D, p. 6, NASA, Washington, DC, August 1, 1991. Reflector ohmic losses, main reflector leakage, and scattering from the subreflector support structure based on estimated values at 2.295 GHz and 8.45 GHz from W. Veruttipong and D. Bathker, JPL Interoffice Memorandum (unnumbered, internal document), Jet Propulsion Laboratory, Pasadena, California, February 7, 1992.

[6] The gain calculations include the following: illumination efficiency, reflector spillover loss, reflector ohmic loss, reflector surface RMS loss, main reflector leakage, BWG return loss, subreflector support structure blockage, reflector alignment loss, horn ohmic loss, horn return loss, and pointing squint. The values for all losses other than illumination efficiency, spillover losses, and horn losses are based on estimated values at 2.295 GHz and 8.45 GHz from W. Veruttipong and D. Bathker, JPL Interoffice Memorandum (unnumbered, internal document), Jet Propulsion Laboratory, Pasadena, California, February 7, 1992.

[7] The target G/T is for 65-percent aperture efficiency and 25 K noise temperature.

[8] W. Veruttipong and D. Bathker, JPL Interoffice Memorandum (unnumbered, internal document), Jet Propulsion Laboratory, Pasadena, California, February 7, 1992.

References

[1] P.-S. Kildal, "Gaussian Beam Model for Aperture-Controlled and Flareangle-Controlled Corrugated Horn Antennas," *IEE Proceedings*, vol. 135, no. 4, part H, pp. 237–240, August 1988.

[2] B. M. Thomas, G. L. James, and K. L. Greene, "Design of Wide-Band Corrugated Conical Horns for Cassegrain Antennas," *IEEE Transactions on Antennas and Propagation*, vol. AP-34, no. 6, pp. 750–757, June 1986.

[3] G. L. James and B. M. Thomas, "TE_{11} to HE_{11} Cylindrical Waveguide Mode Converters Using Ring-Loaded Slots," *IEEE Transactions on Microwave Theory and Techniques*, vol. MTT-30, no. 3, pp. 278–285, March 1982.

[4] V. Galindo-Israel and R. Mittra, "A New Series Representation for the Radiation Integral with Application to Reflector Antennas," *IEEE Transactions on Antennas and Propagation*, vol. AP-25, no. 5, pp. 631–641, September 1977.

[5] Y. Rahmat-Samii and V. Galindo-Israel, "Shaped Reflector Antenna Analysis Using the Jacobi-Bessel Series," *IEEE Transactions on Antennas and Propagation*, vol. AP-28, no. 4, pp. 425–435, July 1980.

Table 1. Feed-horn design parameters.

Parameter	2.86- to 5.35-GHz horn	5.34- to 10-GHz horn
Mode converter section		
Low-frequency limit, f_L, GHz	2.86	5.159
Output design frequency f_i $(= 1.15 f_L)$, GHz	3.289	5.933
Normalized input radius, $k_i a_1$	2.9	2.9
Normalized converter length, z_i/λ_i	1	1
Conical semiangle, θ_i, deg	6	6
Slot width-to-pitch ratio, δ_i	0.75	0.75
Normalized slot pitch, p_i/λ_i	0.1	0.1
Frequency transition section		
Normalized length, z_t'/λ_i	3	3
Angle transition section		
Normalized length, z_t'/λ_i	1	1
Output flare section		
Conical semiangle, θ_i, deg	11	9.85
Normalized aperture radius, a_o/λ_L	3.44	5.33
Slot width-to-pitch ratio, δ_o	0.75	0.75
Pitch, p_o	0.1	0.1

Table 2. Major RF system requirements.

Parameter	Required value
Noise temperature, K	$\leq$25
Polarization	RCP[a] and LCP[b] (simultaneous)
Instantaneous bandwidth, MHz	$\geq$360
Aperture efficiency, %	$\geq$65
Beam efficiency, %	$\geq$90

[a] Right-circular polarization.

[b] Left-circular polarization.

Table 3. DSS 24 system performance at zenith.

Frequency, GHz	Noise temperature, K	Beam efficiency	Aperture efficiency	Gain, dB	G/T, dB/K	Target G/T, dB/K
2.86- to 5.35-GHz feed horn						
2.86	27.64	0.857	0.774	59.04	44.62	44.31
3.289	25.88	0.877	0.783	60.31	46.18	45.53
3.87	24.21	0.879	0.783	61.72	47.88	46.94
4.54	23.64	0.861	0.788	63.14	49.40	48.33
5.34	23.61	0.881	0.750	64.33	50.60	49.74
5.34- to 10-GHz feed horn						
5.34	25.56	0.810	0.787	64.54	50.46	49.74
5.933	25.03	0.803	0.786	65.45	51.47	50.65
7.1	24.60	0.792	0.767	66.90	52.99	52.21
8.45	22.27	0.803	0.757	68.36	54.88	53.72
10.0	23.30	0.772	0.747	69.76	56.09	55.19

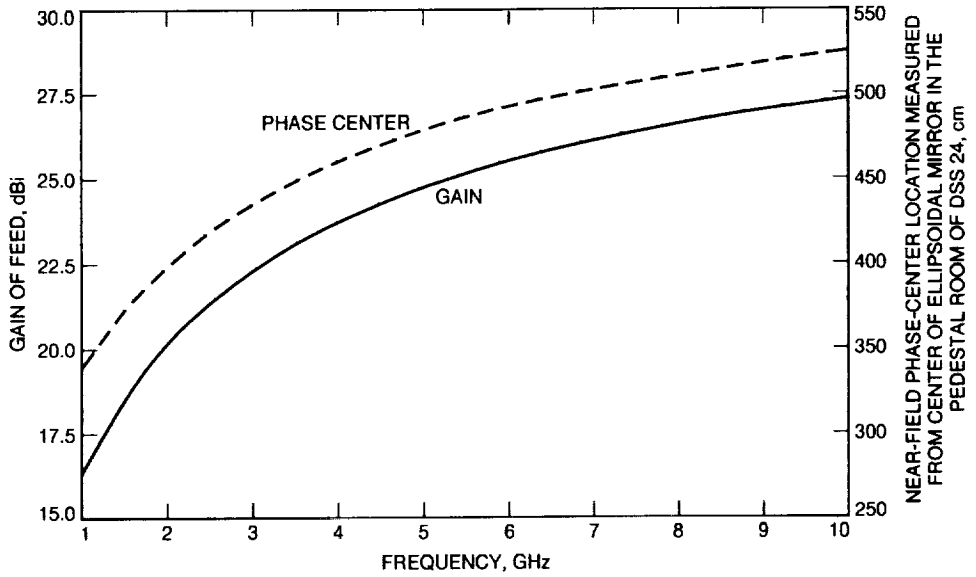

Fig. 1. Initial design gain and near-field phase-center location of feeds for DSS 24.

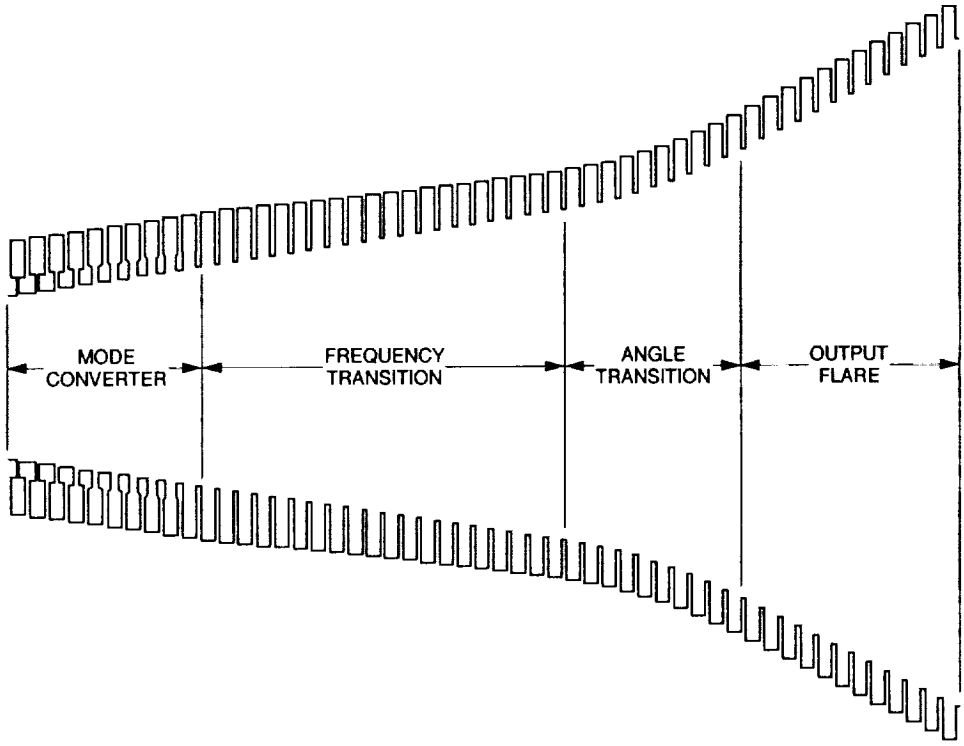

Fig. 2. Basic wideband horn configuration.

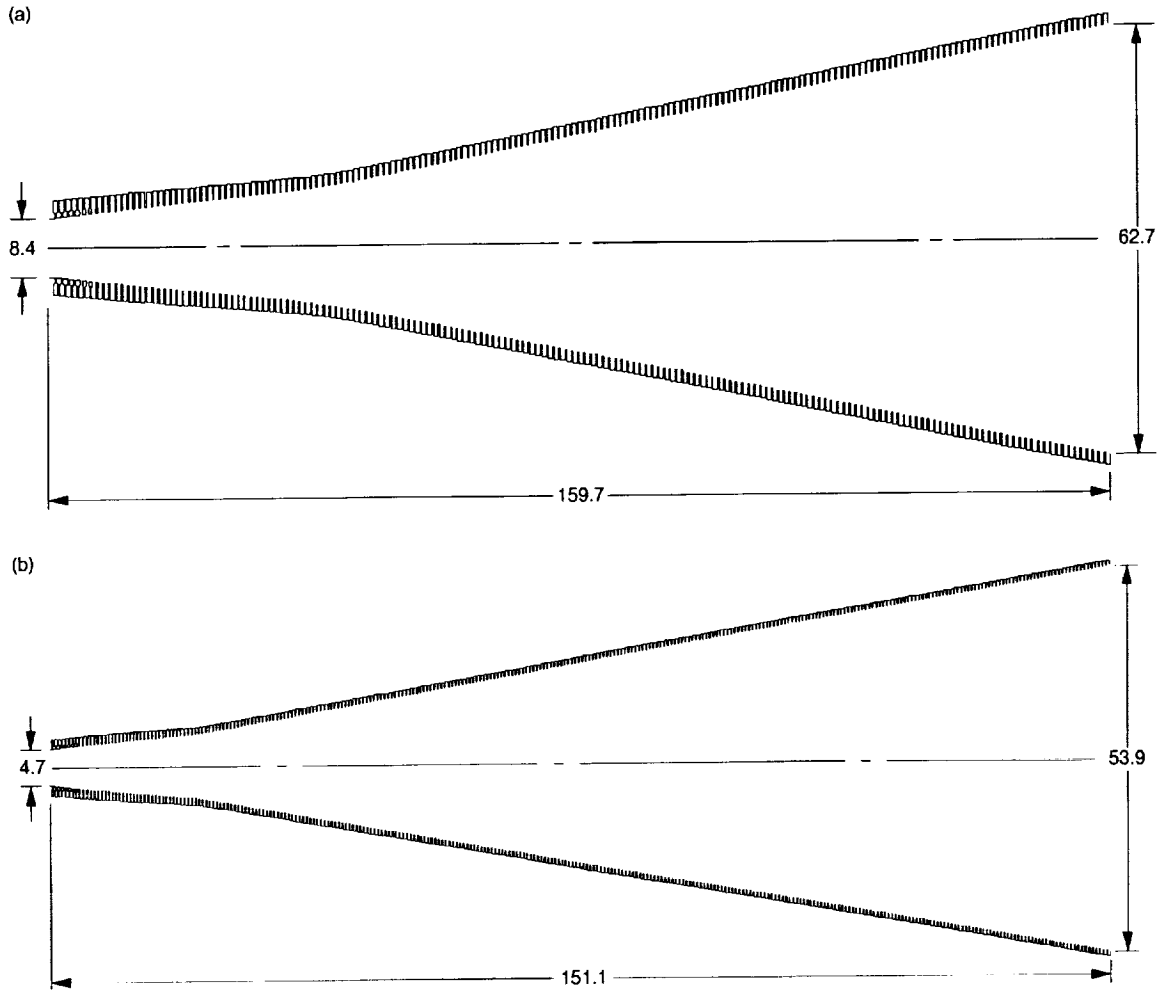

Fig. 3. Profiles of: (a) 2.86- to 5.35-GHz horn and (b) 5.34- to 10-GHz horn.

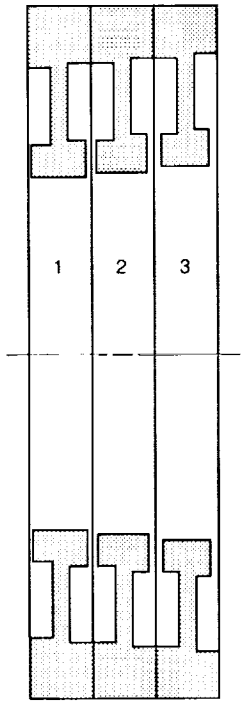

Fig. 4. Cross section of three adjacent mode converter disks.

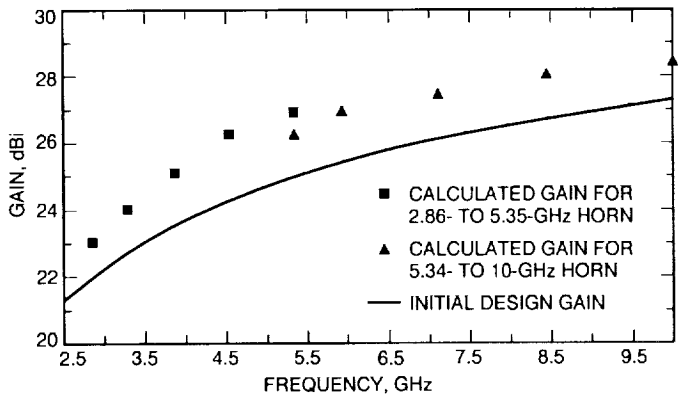

Fig. 5. Calculated horn gain.

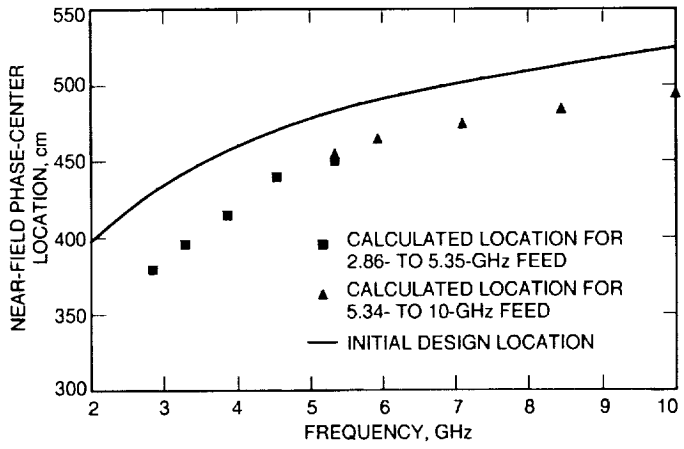

Fig. 6. Calculated near-field phase-center location.

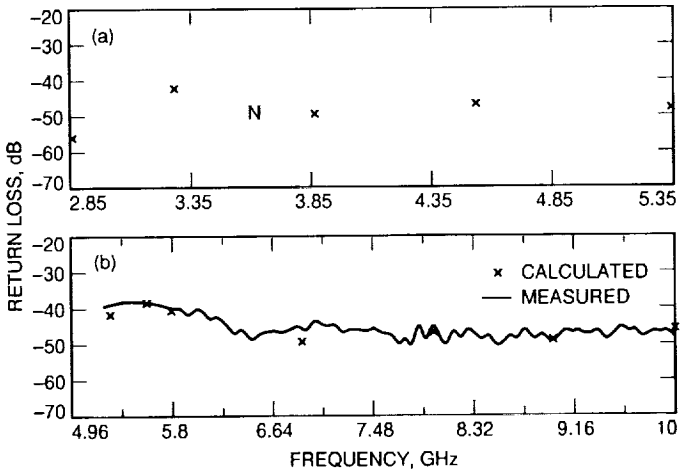

Fig. 7. Return loss of: (a) 2.86- to 5.35-GHz horn and (b) 5.34- to 10-GHz horn.

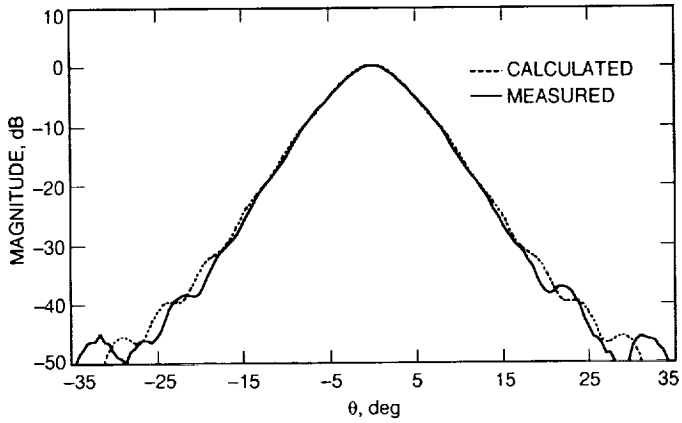

Fig. 8. Far-field copolarization radiation pattern at 7.1 GHz.

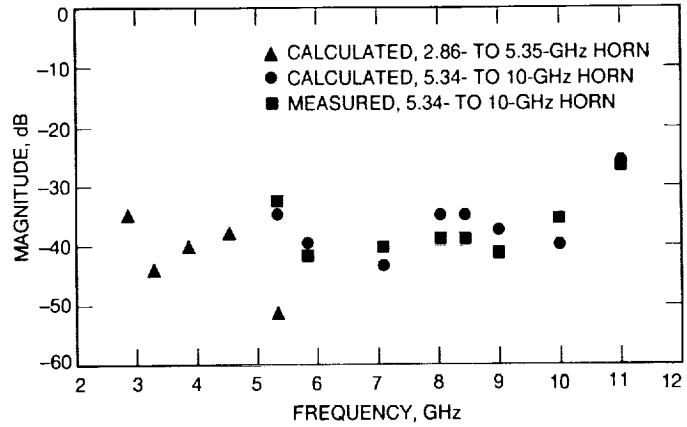

Fig. 9. Maximum cross-polarization of feeds relative to peak copolarization.

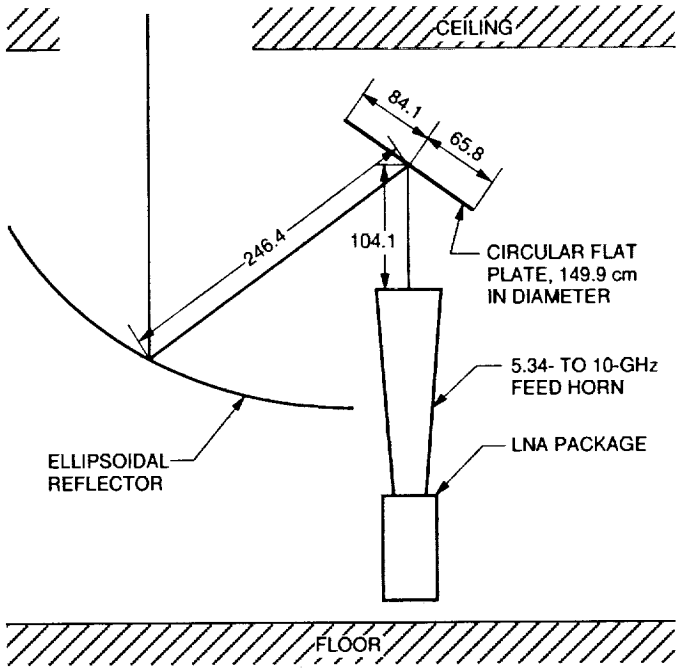

Fig. 10. Flat-plate design for 5.34- to 10-GHz horn.

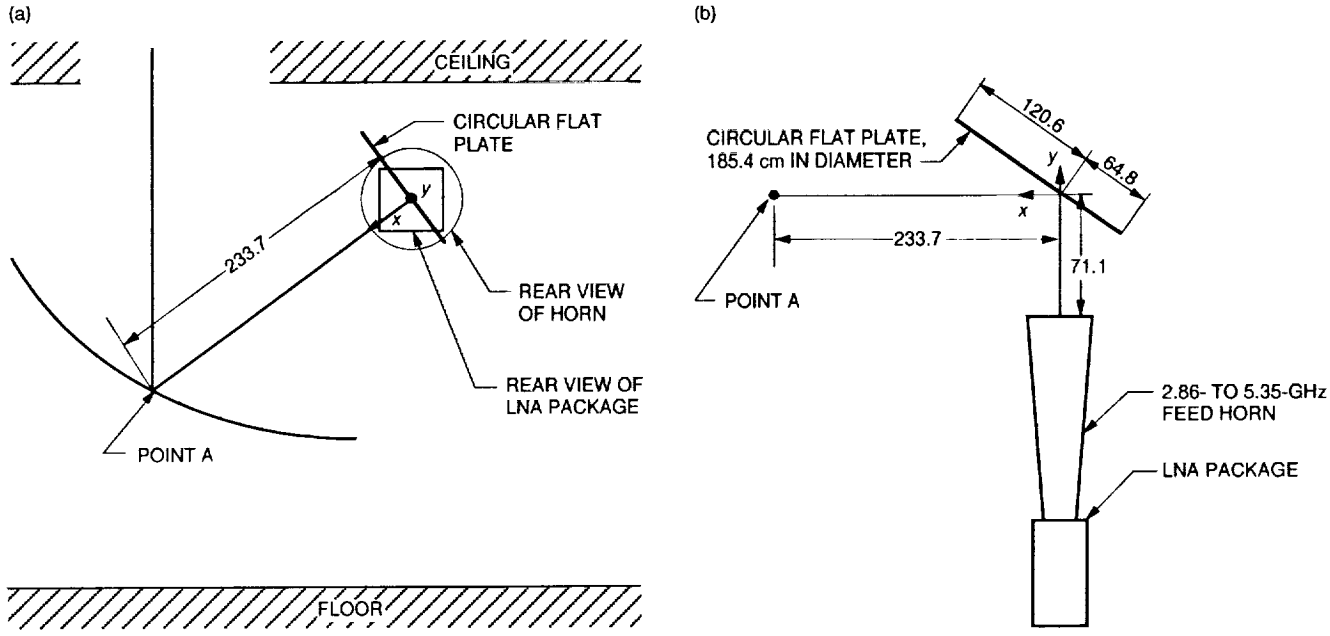

Fig. 11. Flat-plate design for 2.86- to 5.35-GHz horn: (a) rear view and (b) view in *x*, *y* plane.